Dalibor IGREC, Andrej SARJAŠ, Amor CHOWDHURY

University of Maribor

QFT-based robust velocity controller design for a SW-DC motor

Abstract. *The article presents a robust velocity controller design on the basis of Quantitative Feedback Theory for a series-wound DC motor. The aim of this work is to show the design technique with mathematical modelling of a series-wound DC motor, preparation of performance characteristics, selecting QFT boundaries and choosing the controller structure. The controlled system performance obtained with the presented control strategy has been validated through simulation and the results have shown to be consistent with the expected performance of the linear and nonlinear models.*

Streszczenie. *Artykuł przedstawia projekt sterownika prędkości na bazie teorii ilościowego sprzężenia zwrotnego (QFT) dla silnika szeregowego prądu stałego. Celem pracy jest pokazanie techniki projektowania z matematycznym modelem silnika, przygotowanie charakterystyki działania, wyselekcjonowanie ograniczeń QFT oraz wybór struktury sterownika. Działanie systemu sterowanego otrzymane ze strategii działania zostało walidowane przez symulację i rezultaty nie pokazały sprzeczności z oczekiwanym zachowaniem modeli liniowych i nieliniowych. (**Projekt sztywnego sterownika prędkości dla silników szeregowych prądu stałego**)*

Keywords: QFT design, Nichols chart, parameter uncertainty, robust stability
Słowa kluczowe: projektowanie na bazie QFT, wykres Nicholsa, parametr niepewności, stabilność mocna

Introduction

The aim of the modern control feedback theory is to ensure proper and stable system behaviour. Robustness of the closed-loop system to disturbances and uncertainties has always been the central research issue of the feedback control theory. In many cases like electric motors and other open-loop stable systems, feedback would not be needed if there were no disturbances or uncertainties. A simple notation of uncertainties can be presented as the difference between the mathematical model and the real system. Uncertainties mostly have a major ascendancy in the controller design where a linear mathematical model is obtained. Linear mathematical models are more often the result of identification methods [1,2] or linearization of non-linear differential equations, and are merely an imperfect image of the real system. Linear mathematical models thus describe the dynamics of the real system only at one operation condition and with a certain parameters uncertainty.

The analysis of the dynamic performance of an electromotor drive requires the employment of a dynamic model. The model may be either magnetically non-linear with defined parameters in a non-linear manner [5,9,14], or it may be linear [15-17] with either variable [15] or constant [15-17] parameters, depending on the required drive performance and accuracy. A reliable set of motor parameters is essential in many fields: designing control algorithms, automated fault diagnosis and precise simulations. The most common parameters required in such cases are the parameters of a simplified model: stator winding resistance, d-axis reactance and transient reactance, q-axis reactance and transient reactance [3]. In the presented experiment however the mathematical model was obtained analytically. With linearization around several working points we have determined the perturbations of model parameters [4].

For controller design we have selected the method on the basis of the quantitative feedback theory - QFT. QFT is a robust control design procedure that has been developed in the last three decades and is also suitable for SISO and MIMO systems [6]. Its application has also been extended to handling nonlinear and time-varying problems. QFT is probably the only known robust design procedure that simultaneously considers large parametric uncertainty and phase information of closed-loop systems. The ability to satisfy robust stability and different performance constraints with the minimum possible cost of feedback is the biggest advantage of the method over other known robust techniques like μ-synthesis, H_∞ and H_2 [7,8]. The method also offers transparency between the trade-off criteria and the complexity of the controller, where simplicity of the controller structure means a lower possibility of computation error at implementation on a real system.

Modelling of a series-wound DC motor

A series-wound DC motor is one of design variations of the classical brushed DC electric motor with a permanent magnet. The advantage of a series-wound motor is that it develops a larger torque at a low speed. It is well suited for starting heavy loads, and is often used with industrial cranes, winches and elevators, where very heavy loads must be moved slowly and lighter loads more rapidly. As the speed decreases, the torque of a series wound motor increases sharply. When the load is removed from the series motor, the speed will increase sharply. For these reasons, series-wound motors must have a load connected to prevent damage caused by high-speed conditions.

The model of a series-wound brushed DC motor consists of two parts: (1) electrical and (2) mechanical part. The model includes nonlinearities and contains some physical parameters. The values of the physical parameters are not known precisely, and can be subject to some variations. These parameter variations are included as parameter uncertainties [10].

The electrical and the mechanical part of the plant can be expressed with the following equations:

$$u_1 + u_A = \left[R_1 + R_A + \left(L_{11} + L_{AA} \right) p \right] i_A + M_{A1} \dot{\Theta} i_A \tag{1}$$

$$T_L = M_{A1} i_A^2 - Jp\dot{\Theta} - f\dot{\Theta} \tag{2}$$

Rotor resistance R_1 and stator resistance R_A are determined with the UI method by measuring the voltage and the current. We have performed measurements using the recommendations [4]. Measurement of R_A was done at the rotor when the transient voltage at the brush was less than when the rotor rotates. The measured rotor voltage should be empirically increased. Self inductance of stator L_{11} and rotor L_{AA} winding excitation is determined indirectly from the measured responses of both currents at a step voltage change. Both responses are determined separately. The searched inductances are the functions of the corresponding current because of the corresponding magnetic-flux characteristic shape. Therefore they can only be determined for a selected working point [3].

The results of these measurements are nonlinear characteristics of the rotor L_{AA}, stator L_{11} and mutual M_{A1} inductance. All other parameters are used as constants. These are rotor R_1 and stator R_A resistance, rotor inertia J and viscous friction coefficient f.

Nonlinear characteristics of all three nonlinear inductances are shown in figures 1 and 2:

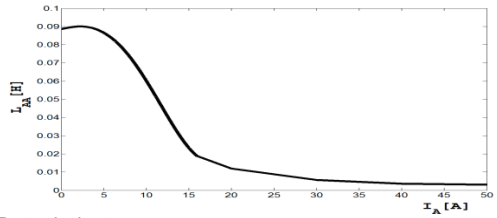

Fig.1. Rotor inductance L_{AA}

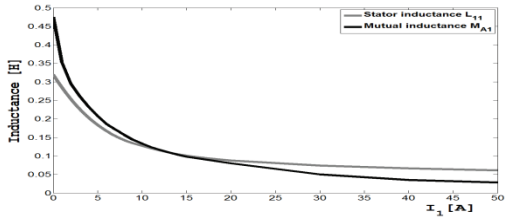

Fig.2. Stator and mutual inductance L_{11}, M_{A1}

Verification of the obtained nonlinear model was done with Matlab-Simulink. Step responses of a nonlinear DC motor model are shown in Figure 3. The gray dotted line is the system response of a nonlinear Simulink DC motor model, while the black line shows the real-system performance. By comparing both responses we have established that the model represents a good approximation to the real-system performance.

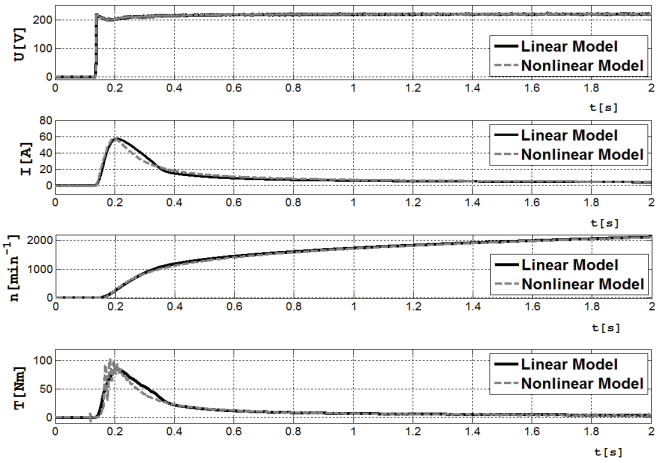

Fig.3. Time responses of a nonlinear DC motor model (gray dotted line) vs. real-time measurements data (black line)

With model linearization and consideration of uncertainties on a set of system working points a family of system linear models was obtained. A linearized motor model around a single working point is described with equations (3) and (4) [3]:

$$u'(s)=\left[R_1+R_A+s\left(L_{11}+L_{AA}\right)+M_{A1}\omega\right]i_A'(s)+ M_{A1}I_A\dot{\Theta}'(s) \tag{3}$$

$$T_L'(s)=2M_{A1}I_Ai_A'(s)-\left(sJ+f\right)\dot{\Theta}'(s) \tag{4}$$

The final linearized model (5) was calculated with equations (3) and (4):

$$\dot{\Theta}'(s)=\frac{2M_{A1}I_Au'(s)-T_L'(s)\left[\left(R_1+R_A\right)+M_{A1}\omega+\left(L_{11}+L_{AA}\right)s\right]}{a_2s^2+a_1s+a_0} \tag{5}$$

$$a_0=fR_1+fR_A+fM_{A1}\omega+2M_{A1}^2I_A^2$$
$$a_1=JR_1+JR_A+JM_{A1}\omega+fL_{11}+fL_{AA}$$
$$a_2=J\left(L_{11}+L_{AA}\right)$$

QFT robust angle velocity controller design

The QFT control design was used to create a simple low-order robust controller for motor-velocity control. The QFT control design has been chosen to achieve reliability and robustness. QFT deals with robust stability margins and robust performance specifications (disturbance rejection, reference tracking, etc.) in the presence of system parameters uncertainty. The QFT approach converts closed-loop system specifications and model uncertainty into a set of constraints or boundaries for every frequency of interest that need to be observed by the nominal open-loop transfer function [11]. Such an integration of information into a set of simple curves in a Nichols chart enables designing the controller by using only a single-nominal-system model. In the controller design stage (loop shaping), the controller is synthesized by adding controller poles and zeros until the nominal loop lies near its boundaries. The optimal controller is obtained when it meets its boundaries and has the minimum high-frequency gain.

We have set the following system performance requirements: 10% or less of overshot on the step response, no steady state error, minimum settling time, minimum rising time, and the system needs to be robustly stabile. Upper and lower boundary tolerances are set as performance criteria (margin specification and tracking specification).

The parameter uncertainty of the system was selected at every frequency of interest (ω_i); with this we got the so-called model-uncertainty templates, which are a set of complex numbers representing the frequency response of the family of uncertain models at a fixed frequency [7].

The controller design procedure involves the following steps: (1) Templates generation and nominal model selection, (2) Performance specifications, (3) QFT boundaries, (4) Loop shaping of the controller C, (5) Pre-filter synthesis F, (6) Simulation and controller design validation.

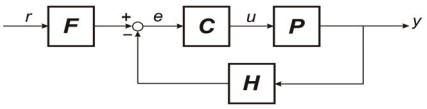

Fig.4. Two-degree of freedom QFT controller structure

The controller C must be designed in such way that the output signal variations y, which are a consequence of the DC motor uncertainties P, are within the specified tolerance boundaries. On the other hand the pre-filter F is designed in order to perform the desired forward control of the reference signal r. The nonlinear system P is converted into a family of linear models.

Linearized DC motor model describes a second-order transfer function with four uncertain coefficients:

$$P(s)=\frac{a_3}{a_2s^2+a_1s+a_0} \tag{6}$$

Coefficients' uncertainty intervals are:

$$a_0\in\left[5.6120\,;\,2.8799\right],\quad a_1\in\left[3.4016\,;\,1.9865\right]$$
$$a_2\in\left[0.0412\,;\,0.0137\right],\quad a_3\in\left[3.5701\,;\,2.5811\right] \tag{7}$$

The nominal model was selected at the working point at $I_A = 8A$ and $n = 1200\ min^{-1}$:

(8) $$P_0(s) = \frac{3.007}{0.02385s^2 + 2.46s + 4.791}$$

The set of critical frequencies was selected around the desired crossover frequency [12]. The frequency domain specifications which the controlled system must fulfil were also given. To determine the closed-loop specifications in the frequency domain we have set up specifications in the time domain and have translated them to the frequency domain:

(9) $$\alpha(\omega) = \left| \frac{856}{(j\omega)^2 + 28.5 \cdot (j\omega) + 855.5} \right|$$

(10) $$\beta(\omega) = \left| \frac{578}{(j\omega)^2 + 99 \cdot (j\omega) + 578} \right|$$

Step responses of the upper $\alpha(\omega)$ and lower $\beta(\omega)$ boundaries in the time domain and their responses translated into the frequency domain are shown in Figures 5a/b.

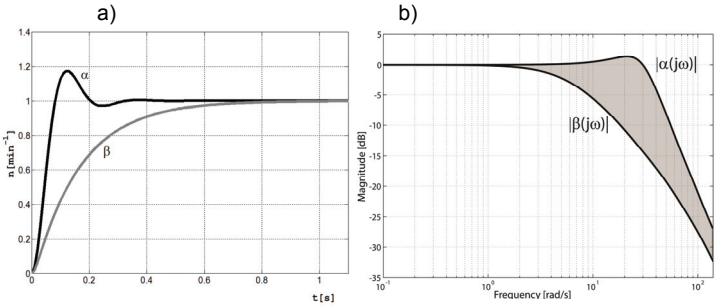

Fig.5a. Specifications in the time domain
Fig.5b. Specifications in the frequency domain

The next step was selecting a frequency array for computing templates and boundaries. For engineering design we need only a small set for a few iterations. The basic rule is that for the same frequency, the boundaries change only with changes in the shape of the template. Therefore, we have looked for frequencies where the distance between the upper and the lower boundary shows significant variations compared to those at other frequencies [10]. These variations are noted as δ_R in Figure 6:

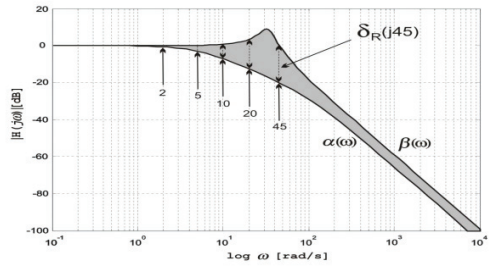

Fig.6. Selected frequency array for computing templates and QFT boundaries

Because the QFT method involves frequency-domain arithmetic, its design procedure requires definition of the plant dynamics only in terms of its frequency responses. The term template is used to denote the collection of an uncertain plant's frequency responses at a selected frequency. Plant template indicates the effect of parameter uncertainties on the gain and the phase of the nominal loop at the given frequency [13]. Plant templates at the chosen frequencies are shown below in Figure 7.

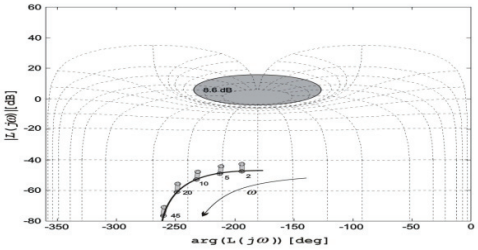

Fig.7. Plant templates

The next step is QFT boundaries calculation. Because the system has to be robustly stabile for each given frequency, the corresponding open-loop response has to be placed right off the corresponding stability boundary. The condition for robust performance is that at each given frequency the corresponding open-loop response is placed above the corresponding performance boundary (Figures 8 and 9).

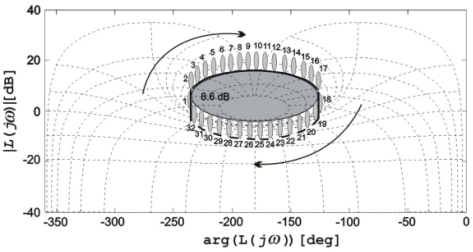

Fig. 8. Robust stability boundaries

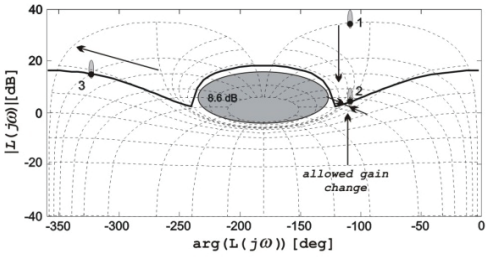

Fig. 9. Robust performance boundaries

With the building elements of the QFT method (controller poles and zeros) the controller was designed so that the open-loop transfer function lies exactly on its robust performance boundaries and does not intersect the stability boundaries at all frequencies. QFT elements are: real pole and zero, complex pole and zero, integrator, lead/lag, complex lead/lag and notch filter. The loop-shaping design is carried out by adjusting, through correct inclusion of QFT elements into the controller structure, the nominal open-loop transfer function $L_0(s)=C(s)P_0(s)$ in the Nichols diagram so that the templates respect the boundaries.

The controller design with the use of loop shaping consists of a few steps. The first step is closing the loop with the controller $C(s)=1$, and setting the gain to $k=1$ (curve A figure 10). Then we add the integrator $1/s$ which eliminates the steady error (figure 10). After that we add two real poles: $1/(s+1.013)$ and $1/(s+25.2)$, which increase the phase margin (curves C and D). In the end we add three real zeros: $(s+0,004)$, $(s+5.56)$ and $(s+12)$ (curves E, F and G). Now the controller has the same numerator and denominator order. By fine tuning the parameters of all added QFT elements we move the curve to the required QFT region (curve H). All curves are presented in Figure 10:

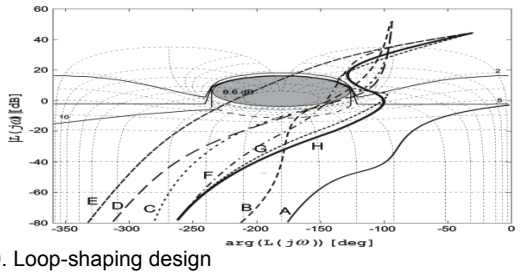

Fig.10. Loop-shaping design

Velocity controller transfer function:

$$C(s)=\frac{88.05(s+12)(s+5.568)(s+0.004019)}{(s+25.2)(s+1.037)s} \tag{11}$$

The pre-filter is used as a part of the QFT design methodology to satisfy the tracking requirements. Region A in Figure 11 shows frequency response immediately after loop shaping. The pre-filter is designed so that the response is manipulated into the tolerance band shown in Figures 11, region B.

Transfer function of the pre-filter:

$$F(s)=\frac{8.1}{s+8.1} \tag{12}$$

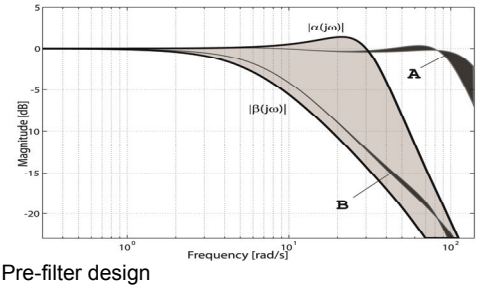

Fig.11. Pre-filter design

The velocity step responses of the controlled system with nonlinear and linearized models are shown in Figure 12.a. Step responses are increased every second by *500 min^{-1}*. The dotted line represents the controlled system response with the nonlinear model, while the black line represents the response with the linearized model. Grey line is the reference signal. A more detailed response in Figure 12.b shows that the nonlinear model response fulfils the requirements. This means that the response is fast, has an overshoot under the limit, and fulfils the requirement of a zero steady state error.

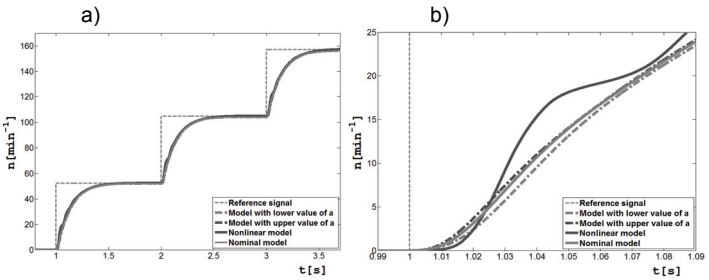

Fig.12 a). Step responses of nonlinear and linearized motor models
Fig.12 b). Step responses of nonlinear and linearized motor models – detailed view

Conclusions

The article presents a robust velocity controller design with the QFT technique for a system with a series-wound DC motor. The robust stability and transient performance requirements are satisfied when applying the QFT controller in the presence of system parameters uncertainty. The major difference between the QFT controller design versus other known robust techniques is that the closed-loop system performance is designated and supervised in every step of the QFT design. The QFT design technique offers transparency of the controller design over robustness and dynamic requirements, where the controller structure is composed of several elements known from the classical control theory, like: lead-lag, lag-lead compensators, integral action and other. Also, it was clear that the obtained controller was simple, robust and of a low order. The main focus of the future research on the QFT controller design will be system energy optimization.

Further work will include adding different loads and disturbances to the nonlinear model as well as testing the controller on a real DC motor.

REFERENCES

[1] Ljung L., System Identification Theory for the user; second edition, Prentice-Hall, New Jersey (1999)

[2] Hadef M., et.al. , Parameter identification of a separately excited DC motor via inverse problem methodology, *Turk J Elec Eng & Comp Sci (*2009), Vol.17, No.2

[3] Aung W. P., Analysis on Modeling and Simulink of DC Motor and its Driving System Used for Wheeled Mobile Robot, *World Academy of Science*, Engineering and Technology 32 (2007)

[4] Dolinar D., et. al., Modeliranje in vodenje elektromehanskih sistemov, *FERI Maribor* (2006)

[5] Hadžiselimović M., et. al. "Magnetically nonlinear dynamic model of synchronous motor with permanent magnets," *J. Magn. Magn. Mater.*, 316 (2007), e257-e260

[6] Horowitz I. M., Quantitative Feedback Design Theory (QFT), *QFT Publications*, Boulder, Colorado, (1993)

[7] Zhou K., et. al., Robust and Optimal Control, Prentice-Hall, New Jersey (1997)

[8] Doyle J. C., et. al., Feedback Control Theory, Macmillan Publishing Co. (1997)

[9] Hadžiselimović M., et. al. "Determining force characteristics of an electromagnetic brake using co-energy," *J. Magn. Magn. Mater.*, 320 (2008), e556-e561

[10] Ackermann J., et. al., Robust Control: Systems with Uncertain Physical Parameters, *Springer-Verlag* (1993)

[11] Borghesani C., et. al., The QFT Frequency Domain Control Design Toolbox, (2001)

[12] Igrec D., Chowdhury A., Svečko R., Uporaba metode QFT " Quantitative Feedback Theory" pri načrtovanju robustnega vodenja, *Elektrotehniški vestnik*, (2008), letn. 75, št. 1/2, str. 37-43

[13] Chen W., Ballanc D. J., Plant Template Generation in Quantitative Feedback Theory, *University of Glasgow* (1998)

[14] Hadžiselimović M., et. al. "Determining parameters of a two-axis permanent magnet synchronous motor dynamic model by finite element method", *Prz. Elektrotech.*, 84 (2008), No. 1, 77-80

[15] Marčič T., et. al. "Modeling of a two-phase synchronous reluctance motor", *Prz. Elektrotech.*, 84 (2008), No. 12, 207-209

[16] Marčič T., et. al. "Determining parameters of a line-start interior permanent magnet synchronous motor model by the differential evolution", *IEEE Trans. Magn.*, 44 (2008), No. 11, 4385-4388

[17] Marčič T., et. al. "Line-Starting Three- and Single-Phase Interior Permanent Magnet Synchronous Motors—Direct Comparison to Induction Motors," *IEEE Trans. Magn.*, 44 (2008), No. 11, 4413-4416

[18] Štumberger B., et. al. "Performance evaluation of synchronous reluctance motor in BLDC drive", *Prz. Elektrotech.*, 85 (2009), No. 12, 147-149

***Authors**: MSc. Dalibor Igrec, E-mail: dalibor.igrec@uni-mb.si; BSc. Andrej Sarjaš E-mail: andrej.sarjas@uni-mb.si; Phd. Amor Chowdhury, E-mail: amor.chowdhury@uni-mb.si; all from University of Maribor, Faculty of Electrical Engineering and Computer Science, Smetanova ulica 17, SI-2000 Maribor, Slovenia.*